IMPROVEMENT VOLTAGE STABILITY OF POWER SYSTEMS WITH SVC'S

[1]*JYOTHILAL NAYAK BHAROTHU*

[1]*Asst.professor & Head, Department of Electrical & Electronics Engineering,*
Columbia Institute of Engineering & Technology, Raipur, C.G; India

ABSTRACT

Voltage stability problems have been one of the major concerns for electric utilities as a result of system heavy loading. The voltage stability problem in electric power systems refers to a range of situations where system operators are unable to keep the voltage profile across the system within adequate operational limits. Its long term causes lie in the imbalance between the growth in demand and the system expansion. The latter may not accompany the former, for example, owing to unpredicted economic constraints. This can cause systems to operate close to their stability limits, very often in conditions for which they were not designed. If a minor contingency occurs in an already stressed system, stability may be lost, leading to the most critical outcome of a voltage instability process: the so-called voltage collapse. After a voltage collapse, the system becomes dismantled owing to the widespread operation of protective devices. This paper presents an artificial neural network (ANN) approach for the advanced load flow models of static VAR compensators (SVC) such as SVC equivalent and firing angle models. These models were incorporated into the Newton-Raphson load flow study. A multi-layered feed forward ANN with error back propagation learning is proposed for the calculation of voltages at the buses, P_{loss}, equivalent SVC value and firing angle value. Extensive testing of the proposed ANN based approach indicates its viability for power system voltages and equivalent SVC value assessment.

Key words: power system, load flow studies, Newton-Raphson, SVC, ANN, VAR

1. INTRODUCTION

1.1 Overview of the Power System

The principal task of Power System operation is to deliver the electric power requested by the customers. This task has to be solved in a safe, reliable and economical manner. The electric power system represents complex system involving many electrical components whose operation must be planned, monitored, analyzed, and controlled. The amount of information to be processed will continue to increase for a number of reasons. Improving power system efficiency and reliability will require increased control system complexity through the addition of new process components.

Present day power systems are being operated closer to their stability limits due to economic and environmental constraints. In Electric power systems, nodal voltages are significantly affected by load variations and by network topology changes. Voltages can drop considerably and even collapse when the network is operating under heavy loading. This may trigger the operation of under-voltage relays and other voltage sensitive controls, leading to extensive disconnection of loads and thus adversely affecting consumers and company revenue. On the other hand, when the load level in the system is low, over-voltages can arise due to Ferranti effect. Capacitive over-compensation and over-excitation of synchronous machines can also occur. Over-voltages cause equipment failures due to insulation breakdown and produce magnetic saturation in transformers, resulting in harmonic generation. Hence, voltage magnitude throughout the network cannot deviate significantly from its nominal value if an efficient and reliable operation of the power system is to be achieved [1].

1.2 Need for the Compensation

Voltage stability has become an increasingly important factor in the operation and planning of electric power systems. Due to the ever-changing operating conditions and various unforeseen factors associated with large power systems, off-line stability studies can no longer ensure a secure operation of the power system [2,3]. On-line stability assessment is based on real-time direct measurements and gives better estimates of power system states and existing topology [4].

A number of tools for voltage stability analysis have been proposed such as P-V curves, V-Q curves, voltage stability indices based on singularity of power flow Jacobian matrix, continuation power flow etc [5].

1.3 Load Flow Studies

Load flow (or power flow) is the solution for the static operating condition of an electric power transmission system, and is the most frequently performed off routine digital-computer power network calculations. Over the last few decades an enormous amount of effort has been expended in research and development on the numerical calculation process. For instance, [6] gives a large but by no means exhaustive bibliography on the subject.

This review will not clearly be unable to cover every aspect of the problem and every proposed solution algorithm, nor is it intended to compete as a catalog of references with other recent sources [6], [7]. Perhaps the most recurrent question arising in the load flow field is which is the best method to choose for a given application? The answer is rarely easy. The relative properties and performances of different load-flow methods can be influenced substantially by the type and size of problem to be solved, by the computing facilities available, and by the precise details of implementation. Any final choice is almost invariably a compromise between the various criteria of goodness by which load-flow methods are to be compared with each other. Every such criterion is directly or indirectly associated with financial cost, in the actual calculation itself, in the engineering application, or in the computer hardware and software requirements. Load-flow calculations are performed in power system planning. They are increasingly being used to solve very large systems, to solve multiple cases for purposes such as outage security assessment, and within more complicated calculations such as optimization and stability.

Prior to, and for some time after, the advent of digital computers, load-flow solutions were obtained using network analyzers. The first really practical automatic digital solution methods appeared in the literature in 1956 and subsequently [8-10]. These Y-matrix iterative methods were well suited to the early generations of computers since they require minimal computer storage. Although they perform satisfactorily on many problems, they converge slowly, and too often not at all. The incentive to overcome this deficiency led to the development of 2-matrix methods [11-13], which converge more reliably but sacrifice some of the advantages of Y-matrix iterative methods, notably storage and speed when applied to large systems. Around the same time, the Newton-Raphson method was shown to have very powerful convergence properties [14], [15], but was computationally uncompetitive. Major breakthroughs in power-system network computation came in the mid-l960, with the development by Tinney and others of very efficient sparsity programmed ordered elimination [16]. One of its earliest successes was in dramatically improving the computing speed and storage requirements of Newton's method, which has now come to be widely regarded as the prominent general-purpose load-flow approach [17], and has been adopted by much of industry. Currently, with the stimulus of increasing problem sizes, on-line applications, and system optimization, newer methods are emerging which are also expected to find wide application.

1.4 Compensation Techniques

Voltage regulation is achieved by controlling the production, absorption and flow of reactive power throughout the network. Reactive power flows are minimized so as to reduce system losses. Sources and sinks of reactive power, such as shunt capacitors, shunt reactors, rotating synchronous condensers and SVC's are used for this purpose. Shunt capacitors and shunt reactors are either permanently connected to the network, or switched on and off according to operative conditions [1].

Advances in power electronics technology together with sophisticated control methods made possible the development of fast SVC's in the early 1970's. The SVC consists of a group of shunt-connected capacitors and reactors banks with fast control action by means of thyristor switching. Problems associated with online implementation of these tools are that they are computationally demanding and need exact mathematical modelling of the system [4].

2.1 Introduction to load flow studies

Load flow calculations provide power flows and voltages for a specified power system subject to the regulating capability of generators, condensers, and tap changing under load transformers as well as specified net interchange between individual operating systems. This information is essential for the continuous evaluation of the current performance of a power system and for effective analyzing of the current performance of a power system expansion to meet increased load flows for both normal and emergency operating conditions.

The load flow problem consists of the calculation of power flows and voltages of a network for specified terminal or bus conditions. A single-phase representation is adequate since power systems are usually balanced. Associated with each bus are four quantities: the real and reactive power, the voltage magnitude, and the phase angle. Three types of buses are represented in the load flow calculation and at a bus, two of the four quantities are specified. It is necessary to select one bus, called the slack bus, to provide the additional real and reactive power to supply the transmission losses, since these are unknown until the final solution is obtained. At this bus the voltage magnitude and phase angle are specified. The remaining buses of the system are designated either as

voltage controlled buses or load buses. The real power and voltage magnitude are specified at a voltage-controlled bus. The real and reactive powers are specified at a load bus.

Network connections are described by using code numbers assigned to each bus. These numbers specify the terminals of transmission lines and transformers. Code number are also used also to identify the types of buses, the location of static capacitors, shunt reactors, and the those network elements in which off-nominal turns ratios of transformers are to be represented.

The two primary considerations in the development of an effective engineering computer program are: (1) the formulation of a mathematical description of the problem; and (2) the application of a numerical method for a solution. The analysis of the problem must also consider the inter-relation between these two factors.

The mathematical formulation of the load flow problem results in a system of algebraic nonlinear equations. These equations can be established by either the bus or loop frame of reference. The coefficients of the equations depend on the selection of the independent variables, i.e., voltages or currents. Thus, either the admittance or impedance network matrices can be used.

Early approaches to the digital solution of load flows employed the loop frame of reference in admittance form. The loop admittance matrix was obtained by a matrix inversion. These methods did not have wide spread application because of the tedious data preparation required to specify the network loops. Furthermore, the required matrix inversion was time-consuming and had to be repeated for each subsequent case involving network changes. Later approaches used the bus frame of reference in the admittance form to describe the system. This method gained widespread application because of the simplicity of data preparation and the ease with which the bus admittance matrix could be formed and modified for network changes in subsequent cases. Also, combinations of voltages and currents have been used as the independent variables. This formulation uses a hybrid matrix consisting of impedance, admittance, current-ratio, and voltage-ratio elements. The ability to formulate efficiently the network matrices has led to the use of the bus frame of reference in the impedance form. However, the majority of load flow programs for large power system studies still employ methods using the bus admittance matrix. This approach remains the most economical from the point of view of computer time and memory requirements.

The solution of the algebraic equations describing the power system is based on an iterative technique because of their non-linearity. The solution must satisfy Kirchhoff's laws, i.e., the algebraic sum of all flows at a bus must equal to zero. One or the other of these laws is used as a test for convergence of the solution in the iterative computational method. Other constraints placed on the solution are: the capability limits of reactive power sources; the tap setting range of tap changing under load transformers; and the specified power interchange between interconnected systems.

2.2 Power System Equations

The equation describing the performance of the network of a power system using the bus frame of reference in impedance form is [18]

$$\bar{E}_{BUS} = Z_{BUS}\bar{I}_{BUS} \qquad (2.1)$$

or in admittance form is

$$\bar{I}_{BUS} = Y_{BUS}\bar{E}_{BUS} \qquad (2.2)$$

The bus impedance and admittance matrices can be formed for the network including the ground bus. The element of the matrices, then, will include the effects of shunt elements to ground such as static capacitors and reactors, line charging, and shunt elements of transformer equivalents. When the ground bus is included and selected as the performance node, the bus voltages in the network performance equations (2.1) and (2.2) are measured with respect to ground.

If the ground bus is not included in the network, the elements of the bus impedance and admittance matrices will not include the effects of shunt elements and one of the buses of the network must be selected as the reference node. In this case, the effects of shunt elements are treated as current sources at the buses of the network and the bus voltages in the performance equations (2.1) and (2.2) are measured with respect to the selected reference bus.

Using the loop frame of reference, the network performance equation in impedance form is

$$\bar{E}_{LOOP} = Z_{LOOP}\bar{I}_{LOOP} \qquad (2.3)$$

or in admittance form is

$$\bar{I}_{LOOP} = Y_{LOOP}\bar{E}_{LOOP} \qquad (2.4)$$

When the loop impedance and admittance matrices are formed for the network not including shunt elements, the dimension of the matrices is $l \times l$, where l is the number of links or basic loops calculated from

$$l = e - n + 1 \qquad (2.5)$$

e is the number of elements, excluding the shunt connections, and n is the number of nodes. In this case, the effects of shunt elements are treated as current sources at the buses of the network.

If the shunt elements e_s are included in forming the loop matrices, the number of elements of the network is increased by e_s. The total number of elements is, then, $e + e_s$ and the number of nodes is increased to $n + 1$. Consequently, the number of loops and the dimension of the loop matrices are increased by $e_s - 1$.

2.3 Power Flow Equations

The real and reactive power at any bus p is [18]

$$P_p + jQ_p = E_p I_p^* \quad \text{or} \quad P_p - jQ_p = E_p^* I_p \tag{2.6}$$

and the current is

$$I_p = \frac{P_p - jQ_p}{E_p^*} \tag{2.7}$$

where I_p is positive when flowing into the system.

In the formulation of the network equation, if the shunt elements to ground are included in the parameter matrix, the total current at bus p is

$$I_p = \frac{P_p - jQ_p}{E_p^*} - y_p E_p \tag{2.8}$$

where y_p is the total shunt admittance at the bus and y_p

E_p is the shunt current flowing from bus p to ground.

After the convergence of the solution, line flows can be calculated. The current at bus p in the line connecting bus p and q is [18]

$$i_{pq} = (E_p - E_q) y_{pq} + E_p \frac{y'_{pq}}{2} \tag{2.9}$$

where y_{pq} = line admittance

y'_{pq} = total line charging admittance

$E_p \frac{y'_{pq}}{2}$ = current contribution at bus p due to line charging

The power flow, real and reactive, is

$$P_p - jQ_p = E_p^* I_{pq} \tag{2.10}$$

$$P_{pq} - jQ_{pq} = E_p^* (E_p - E_q) y_{pq} + E_p^* E_p \frac{y'_{pq}}{2} \tag{2.11}$$

where at bus p the real power flow from bus p to q is P_{pq} and the reactive is Q_{pq}. Similarly, at bus q the power flow from q to p is

$$P_{qp} - jQ_{qp} = E_q^* (E_q - E_p) y_{pq} + E_q^* E_q \frac{y'_{pq}}{2} \tag{2.12}$$

The power loss in line p-q is the algebraic sum of the power flows determined from equations (2.11) and (2.12).

2.4 Newton-Raphson Method

The load flow problem can be solved by the Newton-Raphson method using a set of nonlinear equations to equations to express the specified real and reactive powers in terms of bus voltages. The power at bus p is given by equation (2.6) and the injected current at bus p is given by,

$$I_p = \sum_{q=1}^{n} Y_{pq} E_q \tag{2.13}$$

Substituting from the network performance equation (2.13) for I_p in (2.6),

$$P_p - jQ_p = E_p^* \sum_{q=1}^{n} Y_{pq} E_q \tag{2.14}$$

Since $E_p = e_p + jf_p$ and $Y_{pq} = G_{pq} - jB_{pq}$, equation (2.14) becomes

$$P_p - jQ_p = (e_p - jf_p)\sum_{q=1}^{n}(G_{pq} - jB_{pq})(e_q + jf_q) \quad (2.15)$$

separating the real and reactive parts.

$$P_p = \sum_{q=1}^{n}\{e_p(e_qG_{pq} + f_qB_{pq}) + f_p(f_qG_{pq} - e_qB_{pq})\}$$

$$Q_p = \sum_{q=1}^{n}\{f_p(e_qG_{pq} + f_qB_{pq}) - e_p(f_qG_{pq} - e_qB_{pq})\} \quad (2.16)$$

This formulation results in a set of nonlinear simultaneous equations, two for each bus of the system. The real and reactive powers P_p and Q_p are known and the real and imaginary components of voltages e_p and f_p are unknown for all the buses except the slack bus, where the voltage is specified and remains fixed. Thus there are $2(n-1)$ equations to be solved for a load flow solution.

The Newton-Raphson method requires that a set of linear equations be formed expressing the relationship between the changes in real and reactive powers and the components of bus voltages as follows:

$$\begin{bmatrix} \Delta P_2 \\ \cdots\cdots \\ \Delta P_n \\ \Delta Q2 \\ \cdots\cdots \\ \Delta Q_n \end{bmatrix} = \begin{bmatrix} \frac{\partial P_2}{\partial e_2} & \cdots\cdots & \frac{\partial P_2}{\partial e_n} & \frac{\partial P_2}{\partial f_2} & \cdots\cdots & \frac{\partial P_2}{\partial f_n} \\ \frac{\partial P_n}{\partial e_2} & \cdots\cdots & \frac{\partial P_n}{\partial e_n} & \frac{\partial P_n}{\partial f_2} & \cdots\cdots & \frac{\partial P_n}{\partial f_n} \\ \frac{\partial Q_2}{\partial e_2} & \cdots\cdots & \frac{\partial Q_2}{\partial e_n} & \frac{\partial Q_2}{\partial f_2} & \cdots\cdots & \frac{\partial Q_2}{\partial f_n} \\ \frac{\partial Q_n}{\partial e_2} & \cdots\cdots & \frac{\partial Q_n}{\partial e_n} & \frac{\partial Q_n}{\partial f_2} & \cdots\cdots & \frac{\partial Q_n}{\partial f_n} \end{bmatrix} \begin{bmatrix} \Delta e_2 \\ \cdots\cdots \\ \Delta e_n \\ \Delta f_2 \\ \cdots\cdots \\ \Delta f_n \end{bmatrix} \quad (2.17)$$

where the coefficient matrix is the Jacobian and nth bus is the slack.

$$\begin{bmatrix} \Delta P \\ \Delta Q \end{bmatrix} = \begin{bmatrix} J_1 & J_2 \\ J_3 & J_4 \end{bmatrix} \begin{bmatrix} \Delta e \\ \Delta f \end{bmatrix} \quad (2.18)$$

Equations for determining the elements of the Jacobian can be derived from the bus power equations. The real power from equation (2.15) is

$$P_p = e_p(e_pG_{pp} + f_pB_{pp}) + f_p(f_pG_{pp} - e_qB_{pp}) + \sum_{\substack{q=1 \\ q\neq p}}^{n}\{e_p(e_qG_{pq} + f_qB_{pq}) + f_p(f_qG_{pq} - e_qB_{pq})\}$$

Where p=1,2,…..,n-1 (2.19)

Differentiating, the off-diagonal elements of J_1 are

$$\frac{\partial P_p}{\partial e_q} = e_pG_{pq} - f_pB_{pq} \qquad q \neq p \quad (2.20)$$

and the diagonal elements are

$$\frac{\partial P_p}{\partial e_q} = 2e_pG_{pp} + f_pB_{pp} - f_pB_{pp} + \sum_{\substack{q=1 \\ q\neq p}}^{n}(e_qG_{pq} + f_qB_{pq}) \quad (2.21)$$

However, the equation for the current at bus p is

$$I_p = c_p + jd_p = (G_{pp} - jB_{pp})(e_p + jf_p) + \sum_{\substack{q=1 \\ q\neq p}}^{n}(G_{pq} - jB_{pq})(e_q + jf_q) \quad (2.22)$$

which can be separated into the real and imaginary parts

$$c_p = e_pG_{pp} + f_pB_{pp} + \sum_{\substack{q=1 \\ q\neq p}}^{n}(e_qG_{pq} + f_qB_{pq}) \quad (2.23)$$

$$d_p = f_p G_{pp} - e_q B_{pp} + \sum_{\substack{q=1 \\ q \neq p}}^{n} \left(f_q G_{pq} - e_q B_{pq} \right) \quad p=1,2,\ldots,n-1 \qquad (2.24)$$

Therefore, the expression for the diagonal elements of J_1 can be simplified by substituting the real component of current c_p in equation (2.21) to obtain

$$\frac{\partial P_p}{\partial e_p} = e_p G_{pp} - f_p B_{pp} + c_p \qquad (2.25)$$

From equation (2.19), the off-diagonal elements of J_2 are

$$\frac{\partial P_p}{\partial f_q} = e_p B_{pq} + f_p G_{pq} \quad q \neq p \qquad (2.26)$$

and the diagonal elements of J_2 are

$$\frac{\partial P_p}{\partial f_p} = e_p B_{pp} + 2 f_p G_{pp} - e_p B_{pp} + \sum_{\substack{q=1 \\ q \neq p}}^{n} \left(f_q G_{pq} - e_q B_{pq} \right) \qquad (2.27)$$

The imaginary component of current from equation (2.24) is substituted in (2.28) to obtain

$$\frac{\partial P_p}{\partial f_p} = e_p B_{pp} + f_p G_{pp} + d_p \qquad (2.28)$$

The reactive power from equation (2.16) is

$$Q_p = f_p \left(e_p G_{pp} + f_p B_{pp} \right) - e_p \left(f_p G_{pp} - e_p B_{pp} \right) + \sum_{\substack{q=1 \\ q \neq p}}^{n} \left\{ f_p \left(e_q G_{pq} + f_q B_{pq} \right) - e_p \left(f_q G_{pq} - e_q B_{pq} \right) \right\}$$

p=1,2,….,n-1 (2.29)

Differentiating, the off-diagonal elements of J_3 are

$$\frac{\partial Q_p}{\partial e_q} = e_p B_{pq} + f_p G_{pq} \quad q \neq p \qquad (2.30)$$

and the diagonal elements of J_3 are

$$\frac{\partial Q_p}{\partial e_p} = f_p G_{pp} - f_p G_{pp} + 2 e_p B_{pp} - \sum_{\substack{q=1 \\ q \neq p}}^{n} \left(f_q G_{pq} - e_q B_{pq} \right) \qquad (2.31)$$

The imaginary component of current from equation (2.24) is substituted in equation (2.31) to obtain

$$\frac{\partial Q_p}{\partial e_p} = e_p B_{pp} + f_p G_{pp} - d_p \qquad (2.32)$$

From equation (2.29), the off-diagonal elements of J_4 are

$$\frac{\partial Q_p}{\partial f_q} = -e_p G_{pq} + f_p B_{pq} \quad q \neq p \qquad (2.33)$$

and the diagonal elements of J_4 are

$$\frac{\partial Q_p}{\partial f_p} = e_p G_{pp} + 2 f_p B_{pp} - e_p G_{pp} + \sum_{\substack{q=1 \\ q \neq p}}^{n} \left(e_q G_{pq} + f_q B_{pq} \right) \qquad (2.34)$$

The real component of current from equation (2.24) is substituted in equation (2.34) to obtain

$$\frac{\partial Q_p}{\partial f_p} = -e_p G_{pp} + f_p B_{pp} + c_p \qquad (2.35)$$

Given an initial set of bus voltages, the real and reactive powers are calculated from equation (2.16). The changes in power are the differences between the scheduled and calculated values

$$\Delta P_p^{\,k} = P_{p(scheduled)} - P_p^{\,k} \qquad (2.36)$$

$$\Delta Q_p^{\,k} = Q_{p(scheduled)} - Q_p^{\,k} \quad p=1,2,\ldots,n-1 \qquad (2.37)$$

The estimated bus voltages and calculated powers are used to compute bus currents in order to evaluate the elements of the Jacobian. The linear set of equations (2.17) can be solved for Δe_p and Δf_p, p=1, 2,…,n-1, by a direct or iterative method. Then the new estimates for bus voltages are

$$e_p^{k+1} = e_p^k + \Delta e_p^k \qquad (2.38)$$

$$f_p^{k+1} = f_p^k + \Delta f_p^k \qquad (2.39)$$

The process is repeated until $\Delta P_p^{\,k}$ and $\Delta Q_p^{\,k}$ for all buses are within a specified tolerance.

The Newton-Raphson method can be applied also to solve the load flow problem when the equations are expressed in polar coordinates

$$E_p = |E_p| e^{j\delta_p} \text{ and } Y_{pq} = |Y_{pq}| e^{-j\theta_{pq}}$$

Substituting in equation (2.14), the power at bus p is

$$P_p - jQ_p = \sum_{q=1}^{n} |E_p E_q Y_{pq}| e^{-j(\theta_{pq}+\delta_p-\delta_q)} \qquad (2.40)$$

Since $e^{-j(\theta_{pq}+\delta_p\ \delta_q)} = \cos(\theta_{pq}+\delta_p-\delta_q) - j\sin(\theta_{pq}+\delta_p-\delta_q)$, the real and imaginary components of power are

$$P_p = \sum_{q=1}^{n} |E_p E_q Y_{pq}| \cos(\theta_{pq}+\delta_p-\delta_q) \qquad (2.41)$$

$$Q_p = \sum_{q=1}^{n} |E_p E_q Y_{pq}| \sin(\theta_{pq}+\delta_p-\delta_q) \quad p=1,2,\ldots,n-1 \qquad (2.42)$$

The elements of the Jacobian are calculated from equations (2.41),(2.42) and are

For J_1:

$$\frac{\partial P_p}{\partial \delta_q} = |E_p E_q Y_{pq}| \sin(\theta_{pq}+\delta_p-\delta_q) \quad q \neq p \qquad (2.43)$$

$$\frac{\partial P_p}{\partial \delta_p} = \sum_{\substack{q=1 \\ q\neq p}}^{n} |E_p E_q Y_{pq}| \sin(\theta_{pq}+\delta_p-\delta_q) \qquad (2.44)$$

For J_2:

$$\frac{\partial P_p}{\partial |E_q|} = |E_p Y_{pq}| \cos(\theta_{pq}+\delta_p-\delta_q) \quad q \neq p \qquad (2.45)$$

$$\frac{\partial P_p}{\partial |E_p|} = 2|E_p Y_{pp}| \cos(\theta_{pq}) + \sum_{\substack{q=1 \\ q\neq p}}^{n} |E_q Y_{pq}| \sin(\theta_{pq}+\delta_p-\delta_q) \qquad (2.46)$$

For J_3:

$$\frac{\partial Q_p}{\partial |\delta_q|} = |E_p E_q Y_{pq}| \cos(\theta_{pq}+\delta_p-\delta_q) \quad q \neq p \qquad (2.47)$$

$$\frac{\partial Q_p}{\partial |\delta_p|} = \sum_{\substack{q=1 \\ q\neq p}}^{n} |E_p E_q Y_{pq}| \cos(\theta_{pq}+\delta_p-\delta_q) \qquad (2.48)$$

For J_4:

$$\frac{\partial Q_p}{\partial |E_q|} = |E_p Y_{pq}| \sin(\theta_{pq}+\delta_p-\delta_q) \quad q \neq p \qquad (2.49)$$

$$\frac{\partial Q_p}{\partial |E_p|} = 2|E_p Y_{pp}| sin(\theta_{pp}) + \sum_{\substack{q=1 \\ q \neq p}}^{n} |E_q Y_{pq}| sin(\theta_{pq} + \delta_p - \delta_q) \quad (2.50)$$

Then the equations relating the changes in power to the changes in the voltage magnitudes and phase angles for the Newton-Raphson method is

$$\begin{bmatrix} \Delta P \\ \Delta Q \end{bmatrix} = \begin{bmatrix} J_1 & J_2 \\ J_3 & J_4 \end{bmatrix} \begin{bmatrix} \Delta \delta \\ \Delta |E| \end{bmatrix}$$

2.5 Introduction to Static VAR Compensators

The need to control reactive power through transmission and distribution lines has been recognized since the emergence of the AC power system. Banks of fixed and switched shunt capacitors are used to ensure desirable voltage profile along the transmission and distribution lines. To handle dynamic disturbances such as line switching, loss of generation, load rejection, and system faults, the reactive power has to be supplied quickly to keep the system stable. But the capacitor bank results in a discrete control of reactive power in the system. The thyristor controlled static VAR compensators (SVC) offer such opportunities for dynamic power control. From the late 1970s onwards the SVC has been effectively used to provide a fast and reliable control of production or absorption of reactive power at key locations of the network [19]. SVC's normally include a combination of mechanically controlled and thyristor controlled shunt capacitors and reactors [1].

2.6 Compensation Concepts

Consider the simple two-machine model in Fig. 2.2 for the basic power transfer. The sending end voltage (V_S) and receiving end voltage (V_R) are given by:

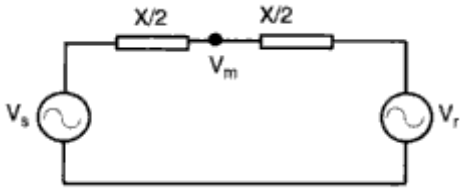

Fig. 2.2 Two-machine system for the analysis

$$V_S = V\left(cos\frac{\delta}{2} + j\, sin\frac{\delta}{2}\right) \quad (2.52)$$

$$V_R = V\left(cos\frac{\delta}{2} - j\, sin\frac{\delta}{2}\right) \quad (2.53)$$

The voltage at the midpoint is:

$$V_M = \left(\frac{V_S + V_R}{2}\right) = V\, cos\left(\frac{\delta}{2}\right) \quad (2.54)$$

The current through the line is given by:

$$I = \left(\frac{V_S \quad V_R}{jX}\right) = \frac{2V}{X} sin\left(\frac{\delta}{2}\right) \quad (2.55)$$

The relation between V_S, V_R, and I is shown in the phasor diagram, Fig. 2.3. If a line without any loss is assumed, the power delivered is:

$$P = \frac{V^2}{X} sin\,\delta \quad (2.56)$$

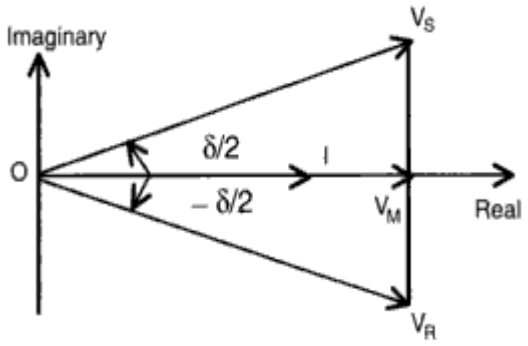

Fig 2.3 Phasor diagram showing the relationship between V_S, V_R and I

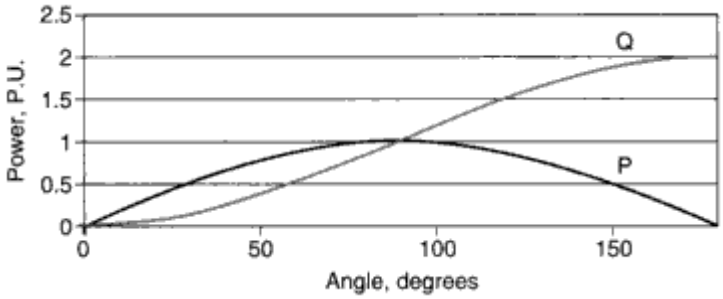

Fig. 2.4 Power angle diagram

The reactive power entering at each end of the line is:

$$Q_S = Q_R = \frac{V^2}{X}(1 - \cos\delta) \qquad (2.57)$$

The total reactive power is:

$$Q = 2Q_S = \frac{2V^2}{X}(1 - \cos\delta) \qquad (2.58)$$

The relationship between P, Q, and δ is plotted in Fig. 2.4. The maximum real power limit is 1.0 P.U. and the maximum reactive power limit is 2.0 P.U.

2.7 Effect of Shunt Compensation

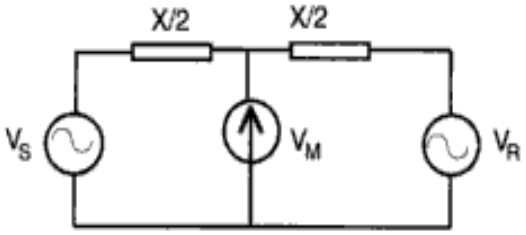

Fig. 2.5 Two-machine system with the compensation at the midpoint

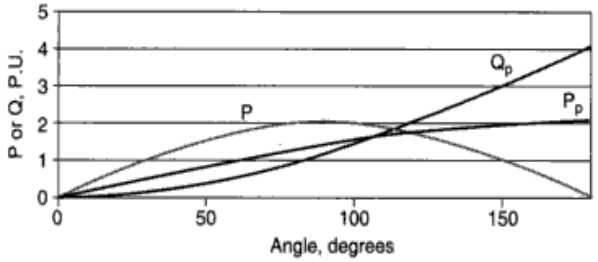

Fig. 2.6 P and Q of the compensated scheme

If a controllable synchronous voltage source is connected at the midpoint, then the reactive power loss can be compensated. Such reactive compensation will increase the real power transmission capability as well. This concept is shown in Fig. 2.5. If the voltage at the midpoint is kept the same as the sending end voltage then the real power P_c is:

$$P_c = \frac{2V^2}{X} \sin\frac{\delta}{2} \qquad (2.59)$$

The corresponding reactive power relation is:

$$Q_c = \frac{4V^2}{X}\left(1 - \cos\frac{\delta}{2}\right) \qquad (2.60)$$

The power and the reactive power plots are shown in Fig. 2.6. This example demonstrates the effect of shunt compensation. In lines with losses, the maximum P and Q will be significantly less. The maximum power transmission in the uncompensated line P occurs at 90°. The maximum power and reactive power of the compensated line occurs at the 180° position.

Synchronous condenser and shunt capacitors provide shunt compensation. The following SVCs are used to provide dynamic shunt compensation.

- Thyristor controlled reactor and fixed capacitor
- Thyristor controlled reactor and thyristor switched capacitor
- Thyristor controlled reactor and mechanically switched capacitor
- Thyristor switched capacitor
- Microprocessor-based SVC

The required type of SVC is selected [20] based on application requirements and cost.

2.8 Description of an SVC

A typical SVC includes thyristors with control circuits, a cooling system for thyristor heat sinks, electronic control equipment, capacitor banks, filter reactors, power circuit breakers, and mounting racks [21]. The thyristors are still low or medium voltage devices and hence the SVCs are manufactured at low or medium voltage levels. In the microprocessor-based SVCs, the thyristor switched capacitor and thyristor controlled reactor are present along with the intelligent control. Usually an interfacing transformer connects the device to a high voltage power system.

2.8.1 Thyristor Controlled Reactor (TCR) and Fixed Capacitor (FC)

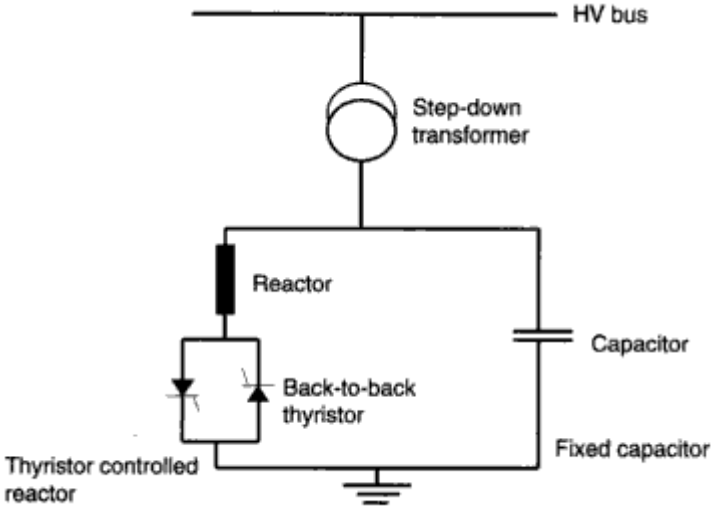

Fig. 2.7 Thyristor Controlled Reactor (TCR) and Fixed Capacitor (FC)

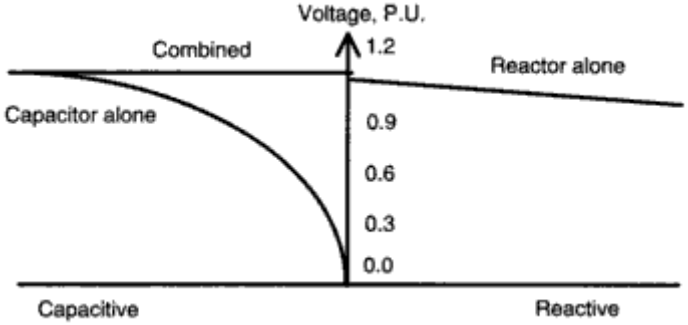

Fig. 2.8 Voltage characteristics with a fixed capacitor and a controlled reactor

In this scheme, the capacitors are usually selected to provide the maximum reactive power needed at the point installation. The required inductive power is dynamically controlled to maintain the desired voltage profile when the demand for reactive power is less than the maximum. The control is performed through phase angle variation. A typical scheme is shown in Fig. 2.7. The result of this compensation is a power factor of nearly unity, with minimum voltage changes due to continuous phase control on the reactor. At maximum leading VAR, the switch is open and the current in the reactor is zero. As the firing angle increases, the harmonic content increases. A 10 MVAR unit typically consists of 10 MVAR of capacitor bank and 10 MVAR of reactor in addition to the thyristor controls. The variation of inductive, capacitive VARS with the system voltage is shown in Fig. 2.8.

3.1 Introduction

In a power system, shunt compensation techniques such as static VAR compensators (SVCs) were placed at some particular buses to obtain the voltage stability. For this two different SVC models were specified. The conventional method includes the Newton Raphson load flow run by incorporating these SVC models. Artificial neural networks (ANNs) are trained with the data obtained from the conventional method using back propagation learning algorithm. Now the results obtained from the ANN were compared with that of the conventional method.

3.2 SVC Equivalent models

The SVC is taken to be a continuous, variable-shunt susceptance, which is adjusted in order to achieve a specified voltage magnitude while satisfying constraint conditions.

Two models are presented in this paper:

1) SVC total susceptance model. A changing susceptance B_{SVC} represents the fundamental frequency equivalent susceptance of all shunt modules making up the SVC. This model is an improved version of SVC models currently available in open literature.

2) SVC firing angle model. The equivalent susceptance B_{eq}, which is function of a changing firing angle α , is made up of the parallel combination of a thyristor-controlled reactor (TCR) equivalent admittance and a fixed capacitive susceptance. This is a new and more advanced SVC representation than those that are currently available in open literature. This model provides information on the SVC firing angle required to achieve a given level of compensation.

The SVC consists of a group of shunt-connected capacitors and reactors banks with fast control action by means of thyristor switching. From the operational point of view, the SVC can be seen as a variable shunt reactance that adjusts automatically in response to changing system operative conditions. Depending on the nature of the equivalent SVC's reactance, i.e., capacitive or inductive, the SVC draws either capacitive or inductive current from the network. Suitable control of this equivalent reactance allows voltage magnitude regulation at the SVC point of connection. SVC's achieve their main operating Characteristic at the expense of generating harmonic currents and filters are employed with this kind of devices. SVC's normally include a combination of mechanically controlled and thyristor controlled shunt capacitors and reactors [31,32]. The most popular configuration for continuously controlled SVC's is the combination of either fix capacitor and thyristor controlled reactor or thyristor switched capacitor and thyristor controlled reactor [33,34]. As far as steady-stale analysis is concerned, both configurations can be modelled along similar lines. The SVC structure shown in Fig.4.1 is used to derive a SVC model that considers the TCR firing angle (α as state variable. This is a new and more advanced SVC representation than those currently available in open literature.

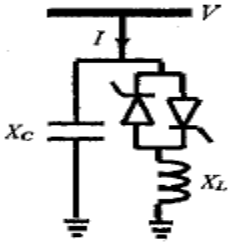

Fig.3.1 SVC Structure

The variable TCR equivalent reactance, X_{Leq}., at fundamental frequency, is given by [33],

$$X_{Leq} = X_L \frac{\pi}{2(\pi - \alpha) + sin(2\alpha)} \qquad (3.1)$$

Where α is the firing angle of the thyristor.

The SVC effective reactance X_{eq} is determined by the parallel combination of X_C; and $X_{Leq,}$

$$X_{eq} = \frac{X_L X_C}{\frac{X_C}{\pi}\left(2(\pi - \alpha) + sin(2\alpha)\right) - X_L} \qquad (3.2)$$

Depending on the ratio X_C/X_L there is a value of firing angle that causes a steady-state resonance to occur. Fig.4.2 depicts the SVC equivalent impedance at the fundamental frequency as function of firing angle, corresponding to a capacitive reactance of 15Ω and a variable inductive reactance of 2.56Ω.

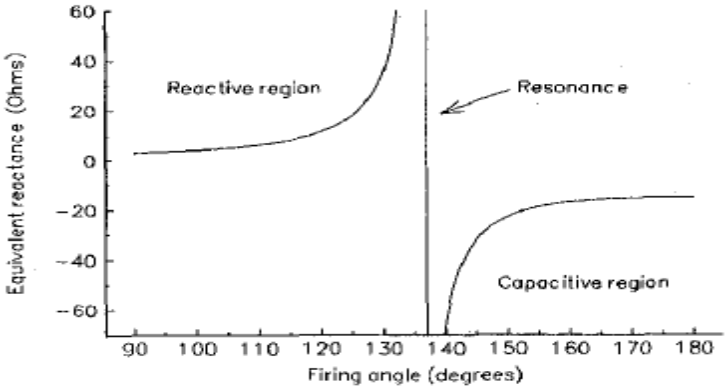

Fig.3.2 SVC equivalent reactance as function of firing angle

The SVC equivalent susceptance is given by (3.3) whilst its profile, as function of firing angle, is given in Fig.3.3.

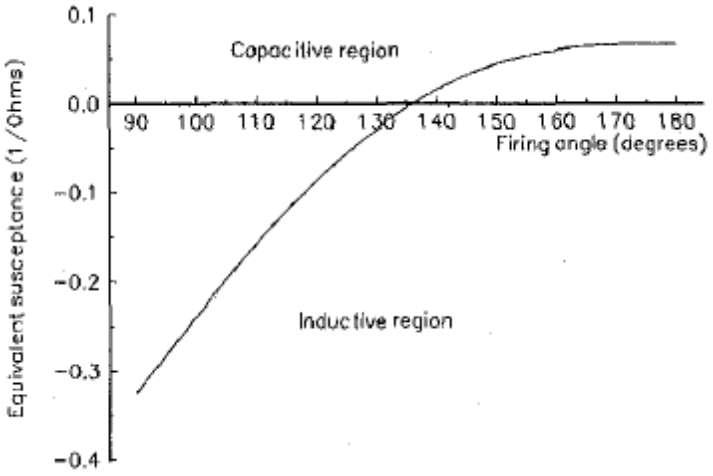

Fig.3.3 SVC equivalent susceptance as function of firing angle

$$B_{eq} = \frac{X_L - \frac{X_C}{\pi}\left(2(\pi - \alpha) + sin(2\alpha)\right)}{X_C X_L} \qquad (3.3)$$

It is shown in Fig.4.3 that the SVC equivalent susceptance profile, as function of firing angle, does not present discontinuities, i.e., B_{eq} varies in a continuous, smooth fashion in both operative regions. Hence, linearization of the SVC power flow equations, based on B_{eq} with respect to firing angle, will exhibit a better numerical behavior than the linearized model based on X_{eq} .

3.3 SVC Load Flow Models

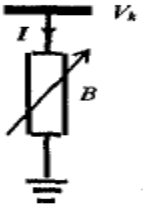

Fig.3.4 Variable shunt susceptance

In practice the SVC can be seen as an adjustable reactance with either firing angle limits or reactance limits. The circuit shown in Fig.4.4 is used to derive the SVC's nonlinear power equations and the linearized equations required by Newton's method.

In general, the transfer admittance equation for the variable shunt compensator is,

$$I = jBV_k \quad (3.4)$$

and the reactive power equation is,

$$Q_k = -V_k^2 B \quad (3.5)$$

3.3.1 SVC Total Susceptance Model ($B = B_{SVC}$)

The linearized equation of the SVC is given by (4.6), where the total susceptance B_{SVC} is taken to be the state variable,

$$\begin{bmatrix} \Delta P_k \\ \Delta Q_k \end{bmatrix}^i = \begin{bmatrix} 0 & 0 \\ 0 & Q_k \end{bmatrix}^i \begin{bmatrix} \Delta\theta_k \\ \frac{\Delta B_{SVC}}{B_{SVC}} \end{bmatrix} \quad (3.6)$$

At the end of iteration i, the variable shunt susceptance B_{SVC} is updated as,

$$B_{SVC}^{i+1} = B_{SVC}^i + \left(\frac{\Delta B_{SVC}}{B_{SVC}} \right)^i B_{SVC}{}^i \quad (3.7)$$

This changing susceptance represents the total SVC susceptance necessary to maintain the nodal voltage magnitude at the specified value.

Once the level of compensation has been determined, the firing angle required to achieve such compensation level can be calculated. This assumes that the SVC is represented by the structure shown in Fig.3.1. Since the SVC susceptance given by (3.3) is a transcendental equation, the computation of the firing angle value is determined by iteration.

3.3.2 SVC Firing Angle Model ($B = B_{eq}$)

Provided the SVC can be represented by the structure shown in Fig.3.1, it is possible to consider the firing angle to be the state variable. In this case, the linearized SVC equation is given as,

$$\begin{bmatrix} \Delta P_k \\ \Delta Q_k \end{bmatrix}^i = \begin{bmatrix} 0 & 0 \\ 0 & \frac{\partial Q_k}{\partial \alpha} \end{bmatrix}^i \begin{bmatrix} \Delta\theta_k \\ \alpha \end{bmatrix}^i \quad (3.8)$$

where

$$\frac{\partial Q_k}{\partial \alpha} = \frac{2V_k^2}{X_L}\left(\cos(2\alpha) - 1\right) \quad (3.9)$$

At the end of iteration i, the variable firing angle α is updated as

$$\alpha^{i+1} = \alpha^i + \Delta\alpha^i \quad (3.10)$$

and the new SVC susceptance B_{eq} is calculated from (4.3).

It should be remarked that both models, the total susceptance model and the firing angle model observe good numerical properties. However, the former model requires of an additional iterative procedure, after the load flow solution has converged, to determine the tiring angle. These models were developed to satisfy similar requirements, but different parameters are adjusted during the iterative process. Hence, their mathematical formulations are quite different. Accurate information about the SVC firing angle, as given by the load flow solution, is of paramount important in harmonics and electromagnetic transients studies [35].

3.3.3 Nodal Voltage Magnitude Controlled by SVC

The implementation of the variable shunt susceptance models in a Newton-Raphson load flow program has required the incorporation of a nonstandard type of bus, namely PVB. This is a controlled bus where the nodal voltage magnitude and active and reactive powers are specified whilst either the SVC's firing angle α or the SVC's total susceptance Bsvc are handled as state variables. If α or Bsvc are within limits, the specified voltage magnitude is attained and the controlled bus remains PVB-type. However, if α or Bsvc go out of limits, they are fixed at the violated limit and the bus becomes PQ-type. This is, of course, in the absence of other FACTS devices capable of providing reactive power support.

3.3.4 Revision of SVC Limits

The revision criterion of SVC limits is based mainly on the reactive power mismatch values at controlled buses. SVC limits revision starts just after the reactive power at the controlled node is less than a specified tolerance. Here this value was set at 10^{-3} p.u.

If the SVC violates limits, the SVC's state variable is fixed at the offending limit. In this case the node is changed from PVB to PQ type. In this situation the SVC will act as an unregulated voltage compensator whose production/absorption reactive power capabilities will be a function of the nodal voltage at the SVC point of connection.

At the end of each iteration, after the network and SVC's state variables have been updated, the voltage magnitudes of all nodes transformed from PVB to PQ type are revised. The purpose of this exercise is to check whether or not it is still possible to maintain the SVC's firing angle or SVC's total susceptance fixed and to check whether or not the node has changed back to the original PVR type without exceeding a or Bsvc limits. The nodal voltage magnitudes of the converted nodes are compared against the specified nodal voltage magnitudes.

The node is reconverted to PVR type if any of the following conditions are satisfied:

1) The SVC violates its upper α or Bsvc limit and the actual nodal voltage magnitude is larger than the specified voltage.
2) The SVC violates its lower α or Bsvc limit and the actual nodal voltage magnitude is lower than the specified voltage.

After the node is returned to PVB type, the voltage magnitude is fixed at the original target value.

3.4 Conventional Method

The location of SVC models during the compensation for voltage support is an important practical question. To answer this question, initially the Newton Raphson load flow was run at the base load and the voltage profile is obtained. Now the load is increased by one percent and the load flow was again run at this load to obtain the voltage profile. The SVC models were placed at those buses where the voltage gradient is high with the load increased by one percent. The test results were obtained for 5, 6 and 14 bus systems with and without SVC models.

3.5 Artificial Neural Network Approach

The ANN with back propagation network using the delta gradient rule is trained with the training patterns that are obtained from the conventional method. Several sets of loads were created by the following scheme:

(a) Varying both the real and reactive power loads simultaneously from 20 to 200% at all the buses of the power system.
(b) Varying only the real power loads from 20 to 200% at all the buses of the power system.
(c) Varying only the reactive power loads from 20 to 200% at all buses of the power system.

These values are obtained at different specified voltage values at the SVC connected node. The k^{th} such load so generated is referred to by the vector X^k and the corresponding output vector, which includes voltage magnitudes of all the buses, P_{loss} and B_{SVC}, is referred as corresponding output vector O^k.

Then the ANN is tested by using some patterns that are not used the training. Now the results were compared for both conventional and ANN approach.

The input vector for the BPN for both the SVC total susceptance model and the SVC firing angle model is the real and reactive power loads at various buses of the power system excluding the slack bus and voltage at the SVC incorporated bus. Thus

$$X = \lfloor P_2, P_3, .., P_N, Q_2, Q_3, .., Q_N, V_{SVC} \rfloor \quad (3.11)$$

Where P_i and Q_i are the active and reactive power loads at bus 'i'.

Vsvc is the voltage to be maintained at the SVC connection point.

The output vector for the BPN for the SVC total susceptance model is the voltage magnitudes at all the buses, P_{loss}, and B_{SVC} value.

$$O = \lfloor V_1, V_2, V_3, .., V_N, P_{loss}, B_{SVC} \rfloor \quad (3.12)$$

Similarly the output vector corresponding to the SVC firing angle model includes the voltage magnitudes at all the buses, P_{loss}, B_{SVC} value and the value of α.

$$O = \lfloor V_1, V_2, V_3, .., V_N, P_{loss}, B_{SVC}, \alpha \rfloor \quad (3.13)$$

The test results were obtained 5, 6 and 14bus systems by also varying hidden neurons in the hidden layer of the BPN.

3.6 Test Results

Newton-Raphson Load Flow Results without SVC

For a 5 bus system,

Bus No.	Voltage	
	Magnitude (p.u.)	Phase angle (degrees)
1	1.0600	0.0000
2	1.0000	-2.0610
3	0.9873	-4.6364
4	0.9841	-4.9567
5	0.9717	-5.7644
P_{loss}	0.0612	

For a 6 bus system,

Bus No.	Voltage	
	Magnitude (p.u.)	Phase angle (degrees)
1	1.0500	0.0000
2	1.1000	-6.8538
3	0.8830	-13.8618
4	0.8710	-10.5723
5	0.8488	-13.9362
6	0.7631	-13.0860
P_{loss}	0.1681	

For a 14 bus system,

Bus No.	Voltage	
	Magnitude (p.u.)	Phase angle (degrees)
1	1.0600	0.0000
2	1.0450	-4.9809
3	1.0100	-12.7180
4	1.0186	-10.3242
5	1.0203	-8.7826
6	1.0700	-14.2227
7	1.0620	-13.3682
8	1.0900	-13.3682
9	1.0563	-14.9466
10	1.0513	-15.1043
11	1.0571	-14.7953
12	1.0552	-15.0774
13	1.0504	-15.1589
14	1.0358	-16.0389
P_{loss}	0.1339	

Newton-Raphson Load Flow Results with SVC equivalent model

For a 5 bus system For a 5 bus system with SVC of 1.06V placed at 5th bus

Bus No.	Voltage	
	Magnitude (p.u.)	Phase angle (degrees)
1	1.0600	0
2	1.0000	-2.1258
3	1.0040	-4.9346
4	1.0057	-5.3371
5	1.0600	-7.2426
bsvc	0.0890	
P_{loss}	0.0843	

For a 14 bus system For a 5 bus system with SVC of 1.06V placed at 14th bus

Bus No.	Voltage	
	Magnitude (p.u.)	Phase angle (degrees)
1	1.0600	0
2	1.0450	-4.9776
3	1.0100	-12.7047
4	1.0199	-10.3380
5	1.0211	-8.7894
6	1.0700	-14.2194

Issue 2 Vol 1 january 2013
ISSN 2319 – 7277

For a 6 bus system For a 5 bus system with SVC of 1.06V placed at 6th bus

Bus No.	Voltage	
	Magnitude (p.u.)	Phase angle (degrees)
1	1.0500	0.0000
2	1.1000	-1.8334
3	1.0044	-12.1527
4	0.9997	-9.6609
5	1.0713	-12.5652
6	1.0600	-12.4555
bsvc	0.2500	
P_{loss}	0.0885	

7	1.0723	-13.3613
8	1.0900	-13.3613
9	1.0554	-14.9324
10	1.0505	-15.0918
11	1.0567	-14.7867
12	1.0582	-15.1188
13	1.0559	-15.3093
14	1.0600	-16.6468
bsvc	0.0142	
P_{loss}	0.1340	

Convergence Characteristics of ANN for SVC Equivalent model

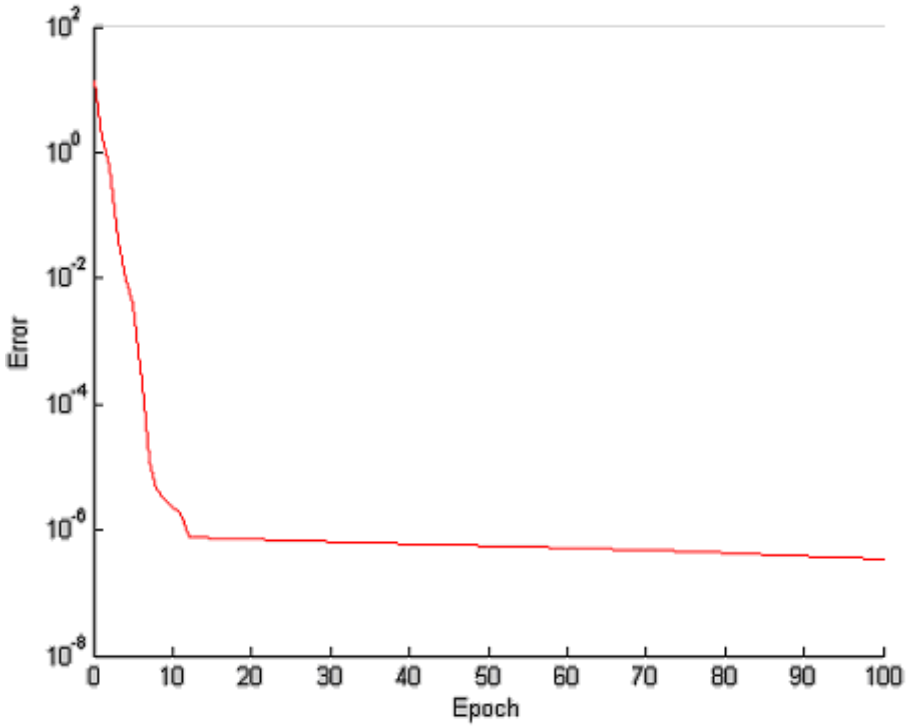

Fig.3.5 Convergence Characteristics of ANN for SVC Equivalent model for 5 bus system
Newton-Raphson Load Flow Results with SVC firing angle model

For a 5 bus system with SVC of 1.06V placed at 5th bus

Bus No.	Voltage	
	Magnitude (p.u.)	Phase angle (degrees)
1	1.0600	0
2	1.0000	-2.1259
3	1.0040	-4.9347
4	1.0057	-5.3372
5	1.0600	-7.2428
bsvc	0.0891	
Alfa	2.2670	
P_{loss}	0.0843	

For a 6 bus system with SVC of 1.06V placed at 6th bus

Bus No.	Voltage	
	Magnitude (p.u.)	Phase angle (degrees)
1	1.0500	0
2	1.1000	-1.8334
3	1.0044	-12.1527
4	0.9997	-9.6609
5	1.0713	-12.5652
6	1.0600	-12.4555
bsvc	0.4451	
Alfa	2.4249	
P_{loss}	0.0885	

For a 14 bus system with SVC of 1.06V placed at 14th bus

Bus No.	Voltage	
	Magnitude (p.u.)	Phase angle (degrees)
1	0	1.0600
2	-4.9786	1.0450
3	-12.7084	1.0100
4	-10.3337	1.0195
5	-8.7845	1.0206
6	-14.2183	1.0700
7	-13.3582	1.0721
8	-13.3582	1.0900
9	-14.9294	1.0552
10	-15.0891	1.0504
11	-14.7847	1.0566
12	-15.1178	-1.0582
13	-15.3085	1.0559
14	-16.6473	1.0600
bsvc	0.0446	
Alfa	2.2502	
P_{loss}	0.1341	

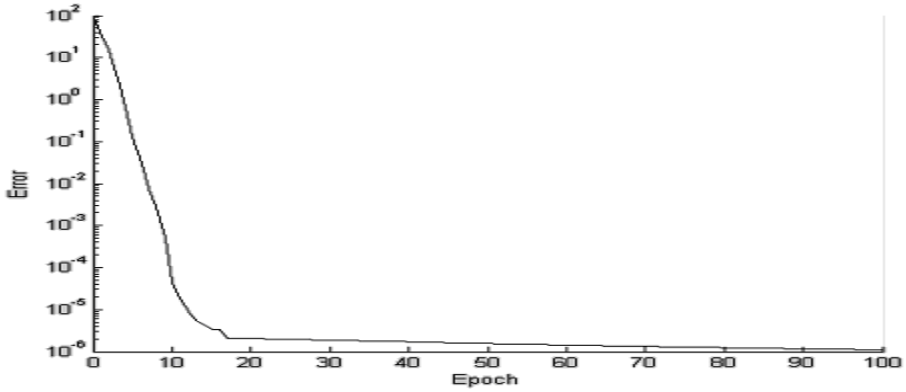

Fig.3.6 Convergence Characteristics of ANN for SVC Equivalent model for 6 bus system

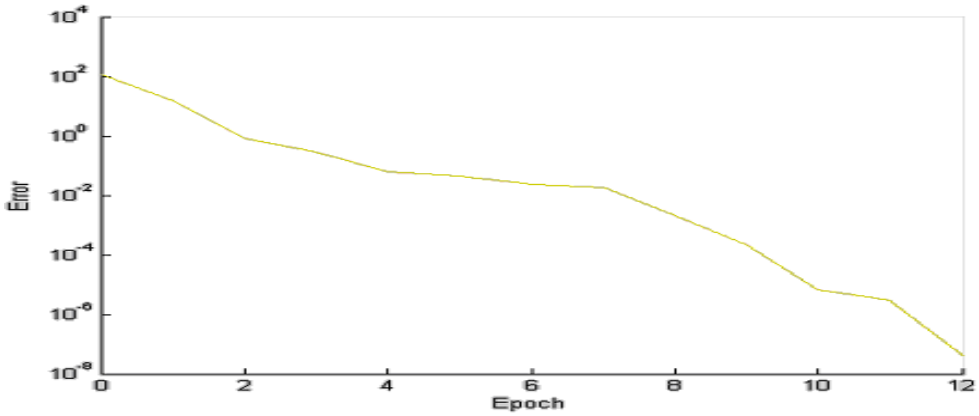

Fig.3.7 Convergence Characteristics of ANN for SVC Equivalent model for 14 bus system

3.6.4 Convergence Characteristics of ANN for SVC firing angle model

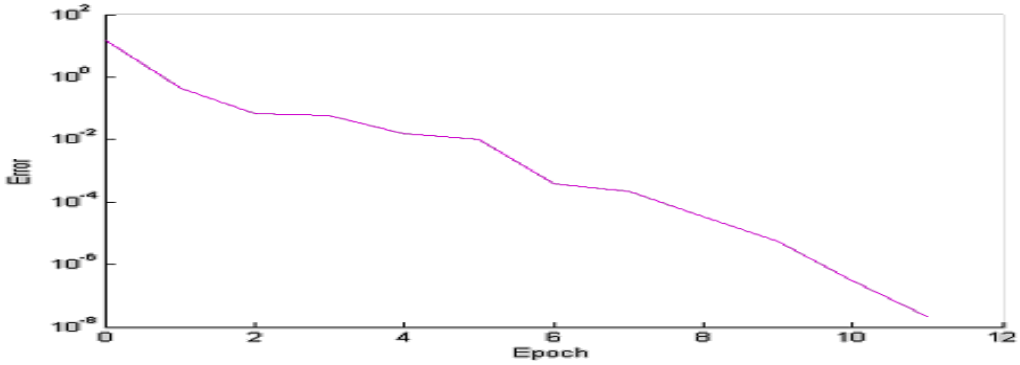

Fig.3.8 Convergence Characteristics of ANN for SVC firing angle model for 5 bus system

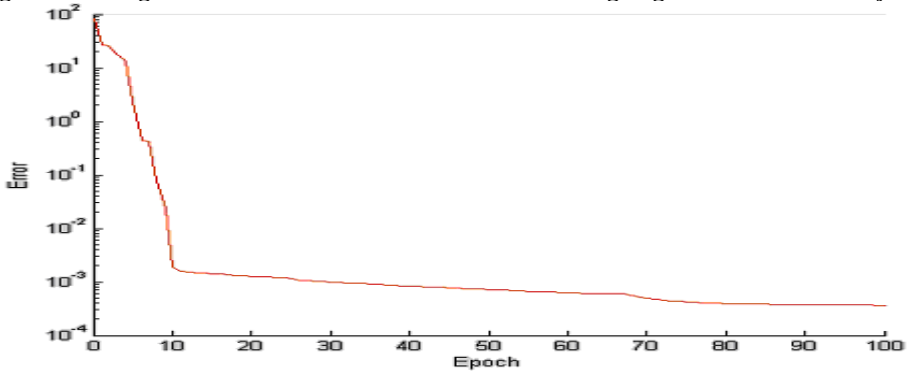

Fig.3.9 Convergence Characteristics of ANN for SVC firing angle model for 6 bus system

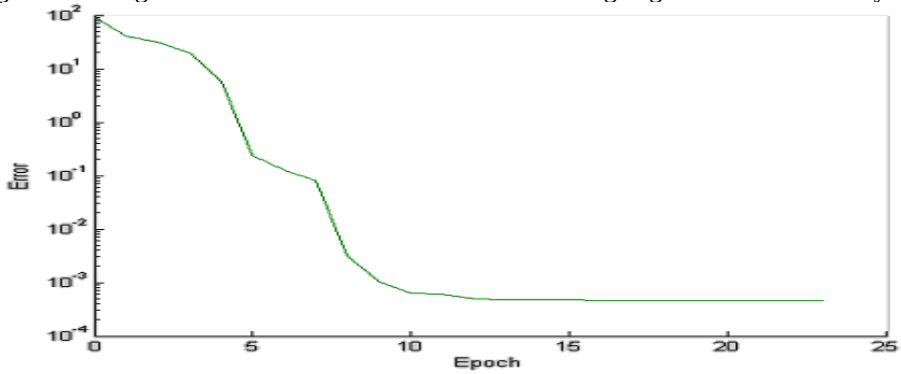

Fig.3.10 Convergence Characteristics of ANN for SVC firing angle model for 14 bus system

ANN Results for SVC Equivalent model

For a 5 bus system with SVC of 1.06V placed at 5th bus and with 18 hidden neurons

Bus No.	Voltage	
	Magnitude (p.u.)	Phase angle (degrees)
1	1.0600	0.0000
2	1.0000	-2.1268
3	1.0040	-4.9363
4	1.0057	-5.3388
5	1.0599	-7.2448
bsvc	0.0885	
P_{loss}	0.0841	

For a 5 bus system with SVC of 1.06V placed at 5th bus and with 60 hidden neurons

Bus No.	Voltage	
	Magnitude (p.u.)	Phase angle (degrees)
1	1.0499	-0.0003
2	1.0998	-1.8337
3	1.0043	-12.1527
4	0.9997	-9.6610
5	1.0715	-12.5652
6	1.0601	-12.4554
bsvc	0.2499	
P_{loss}	0.0883	

For a 5 bus system with SVC of 1.06V placed at 14th bus and with 27 hidden neurons

Bus No.	Voltage	
	Magnitude (p.u.)	Phase angle (degrees)
1	1.0600	0.0000
2	1.04500	-4.9775
3	1.0100	-12.7045
4	1.0200	-10.3378
5	1.0211	-8.7892
6	1.0700	-14.2190
7	1.0723	-13.3611
8	1.0900	-13.3610
9	1.0554	-14.9321
10	1.0506	-15.0915
11	1.0566	-14.9321
12	1.0582	-15.1184
13	1.0559	-15.3089
14	1.0600	-16.6464
bsvc	0.0142	
P_{loss}	0.1340	

ANN Results for SVC firing angle model

For a 5 bus system with SVC of 1.06V placed at 5th bus and with 15 hidden neurons

Bus No.	Voltage	
	Magnitude (p.u.)	Phase angle (degrees)
1	1.0600	0.0000
2	1.0000	-2.1260
3	1.0040	-4.9350
4	1.0057	-5.3375
5	1.6000	-7.2429
bsvc	Bsvc = 0.0889	
Alfa	Alfa = 2.2670	
P_{loss}	ploss = 0.8420	

For a 6 bus system with SVC of 1.06V placed at 6th bus and with 16 hidden neurons

Bus No.	Voltage	
	Magnitude (p.u.)	Phase angle (degrees)
1	1.0500	0.0000
2	1.1013	-1.8526
3	1.0050	-12.1545
4	1.0001	-9.6627
5	1.0723	-12.5504
6	1.0606	-12.4470
bsvc	0.4453	
Alfa	2.4248	
P_{loss}	ploss = 0.0885	

For a 14 bus system with SVC of 1.06V placed at 14th bus and with 33 hidden neurons

Bus No.	Voltage	
	Magnitude (p.u.)	Phase angle (degrees)
1	1.0601	0.0007
2	1.0428	-4.9799
3	1.0069	-12.6970
4	1.0156	-10.3344
5	1.0212	-8.7936
6	1.0693	-14.2367
7	1.0708	-13.3414
8	1.0881	-13.3442
9	1.0548	-14.9084
10	1.0506	-15.0731
11	1.0600	-14.7900
12	1.0622	-15.1297
13	1.0579	-15.3043
14	1.0587	-16.5954
bsvc	0.0450	
Alfa	2.2514	
P_{loss}	0.1348	

CONCLUSIONS

In this paper work, a proto type of ANN is developed to give voltage magnitudes and phase angles at different buses of the system, operating susceptance of the SVC, firing angle value and system losses at that load. This ANN is best suited for online applications to monitor the system voltage profile for that operating load as it gives its response at faster rate which is a required characteristic in the real time applications.

ACKNOWLEDGEMENTS

I am very much thankful to my friend Mr. D Srinivas who helped ANN application for this paper. I Thank to our college principal Dr. TVV Sudhakar for his kind permission and encouragement to write research paper. Also I am very much thankful to our college Chairman Mr. Kishore Jadwani, vice chairman Mr. Vijay Jadwani, Secretary Mr. Harjeet Singh Hura for providing creative environment for this work. I would like to extend my heartfelt thanks to my colleagues. And finally I am very much obliged to my respected parents who inspiring around the clock.

AUTHOR BIOGRAPHY

Jyothilal Nayak Bharothu received the B.E (Electrical &Electronics Engg.) from S.R.K.R Engg. College Bhimavaram (Andhra University) in 2006, and

M.Tech;(Power systems- High Voltage Engg) from JNTU KAKINADA University in 2009. He has five years of teaching experiences in the field of Electrical Engg. In India, his field of interest is power systems operation and control. Presently, he is H.O.D. of EEE Dept at Columbia Institute of Engineering and Technology RAIPUR (C.G.), INDIA

REFERENCES

[1] H. Ambriz-Perez, E. Acha, and C. R. Fuerte-Esquivel, "Advanced SVC models for Newton–Rapshon load flow and Newton optimal power flow studies," IEEE Trans. Power Syst., vol. 15, no. 1, pp. 129–136, Feb. 2000.

[2] PSERC Publication 01-05, "Automated Operating Procedures for Transfer limits". Power Systems Engineering Research Center, Cornell University. Final report. May 2001.

[3] PSERC Publication 03-06. " Integrated Security Analysis", Power System Engineering Research Center, Cornell University, Final report. May 2003.

[4] Saikat Chakrabarti, B.Jeyasurya, "On-line Voltage Stability Monitoring Using Artificial Neural Network," IEEE August 20004.

[5] P.Kundur, Power System Stability and Control, Mcgraw-Hill,1993.

[6] M. R. G. Al-Shakarchi, 'Nodal iterative load flow," M.Sc thesis, University of Manchester Institute of Science and Technology, Manchester, U. K., 1973.

[7] D. A. Comer, "Representative bibliography on load-flow analysis and related topics," presented at the IEEE PES Winter Meet.,New York, Jan 28-Feb. 2,1973. Paper C73-104-7.

[8] J. B. Ward ant H. W. Hale, "Digital computer solution of power flow problems", AIEE Trans. (Power App. Syst.), vol. 75, pp. 398-404, June 1956.

[9] A. F. Glimn and G. W. Stagg, "Automatic calculation of load flows," AIEE Trans. (Power App. Syst.), vol. 76, pp, 817-828, Oct. 1957.

[10] R. J. Brown and W. F. Tinney, "Digital solutions for large power networks," AIEE Trans. (Power App. Syst.), vol. 76, pp. 347-355, June 1957.

[11] P. P. Gupta and M. W. Humphrey Davies, 'Digital computers in power system analysis," Proc. Inst. Elec. Eng., vol. 108A, pp. 383-404, Jan. 1961.

[12] A. Brameller and J. K;, Denmead, "Some improved methods of digital network analysi,", Proc. Inst. Elec. Eng., vol. 109A, pp. 109-116, Feb. 1962.

[13] H. E. Brown, G. K. Carter, H. H. Happ, and C. E. Person, "Power flow solution by impedance matrix iterative method," IEEE Trans. Power App. Syst., vol. PAS-82, pp. 1-10, Apr. 1963.

[14] J. E. Van Ness, "Iteration methods for digital load flow studies," AIEE Trans. (Power App. Syst.), voL 78. pp. 583-588, Aug. 1959.

[15] J. E. Van Nness and J. H. Griffin, "Elimination methods for load flow studies," AIEE Trans. (Power App. Syst.), vol. 80, pp. 299-304, June 1961.